

Magnetic Induction Antenna Arrays for MIMO and Multiple-Frequency Communication Systems

Nikolay Tal*, Yahav Morag, and Yoash Levron

Abstract—In magnetic induction communication systems, channel capacity is often a major bottleneck that limits the system performance. This paper proposes a method to increase the channel capacity in such systems by means of an antenna array. A central challenge in the design of magnetic antenna arrays is to achieve low intra-array coupling along with high gain. These two properties are essential for increasing the channel capacity in comparison to single antenna communication systems of comparable volume. The method proposed in this paper utilizes circular loop antennas to reduce the intra-array coupling using magnetic flux cancellation. The mathematic approach employed in this paper considers each coil as a system of coupled inductors, where each inductor is a single turn loop, and the total coil self and mutual inductances are computed by summing the appropriate single turn loop inductances. Volume efficient coil topologies are identified, and an optimization method is proposed to minimize the intra-array coupling, subject to a required inductance. The proposed method allows to design volume efficient, up to 3×3 , array, or pyramidal shaped 4×4 arrays. The results are verified experimentally using the multiple-frequency communication mode.

1. INTRODUCTION

Magnetic Induction (MI) communication is a promising alternative communication scheme for wide variety of applications, in which it is superior to communication based on classic EM waves. These applications include Body Area Networks (BAN), underground and underwater communication for land sliding and earthquake monitoring, oil reservoirs and pipelines leakage, and more [1–5]. In such applications, the conductivity of earth and water requires low frequencies operation to compensate for the high path loss in the medium, which is proportional to square root of frequency. This in turn requires large antennas. In underground environment, an additional problem is rapid changes in channel conditions due to changing nature of the terrain, which poses significant challenges [6–10].

Magnetic induction (MI) communication systems utilize low frequency near magnetic field to transmit data between the transmitter and the receiver. This technique is weakly affected by the communication medium, as the operation frequency is low, and so the attenuation in conducting medium, and the magnetic permeability of most natural materials is unity [1]. The transmitting coil need not to be an efficient radiator, hence, its size is much smaller than wavelength, enabling practical antenna size at low frequencies. The magnitude of the near field decays at faster rate than far field: r^{-3} compared to r^{-1} . Such rapid decay is advantageous in some applications that operate at a non-conductive environment, as it enables to create secure communication bubbles around the transmitter and promotes frequency reuse [11]. The applicability of MI communication in underground environment depends mainly on the depth of the buried transceivers. At applications in which the transceivers are buried in the shallow depth, the far field EM path loss is lower than the near field, despite higher operation frequency, and in such applications, classic EM communication is advantageous [12]. However,

Received 7 March 2017, Accepted 31 May 2017, Scheduled 8 July 2017

* Corresponding author: Nikolay Tal (nikolayt@campus.technion.ac.il).

The authors are with the Department of Electrical Engineering, Technion-Institute of Technology, Haifa, Israel.

if the transceivers are deeply buried, the MI communication is a viable alternative [12], with lower path loss and constant channel conditions, even for time-varying channels [2, 5, 12].

There are two main challenges associated with magnetic induction communication systems: range and channel capacity. The methods proposed to increase communication range may be divided into two categories: (a) waveguide-based techniques [1, 10, 13–18], and (b) sensitivity increase of the receiver. The waveguide techniques significantly reduce the path loss, and hence increases the communication range compared to ordinary MI systems and EM wave systems [18]. The additional method to increase the communication range, without increasing transmitting power, is improving the sensitivity of the receiver [19–24]. These works focus on general search coil magnetometers, but their results can be employed in optimal design of MI communication receivers as well.

An additional method to increase channel capacity employs arrays of transmitting and receiving antennas. Such technology is widely employed in classic far-field EM communication and is implemented, for example, in devices operating under the 802.11n IEEE standard. In the area of MI communication, the use of antenna arrays was recently analyzed in [25–27]. In [25] the channel capacity of Multiple-Input-Multiple-Output (MIMO) system is analyzed. In [26] a 3×3 MIMO array is proposed with partial intra-array coupling cancellation, which supports increased data rates. The work in [27] proposed a method to design a MI MIMO array with zero intra-array coupling. This cancellation is achieved by using a multiple-pole loop antenna, and is not limited to 2×2 or 3×3 array. Due to self-cancellation occurring in a multiple-pole loop antenna, the gain of quadrupole loop antenna is 9 dB lower than that of the circular loop antenna with same radii of 100 mm, and the gain loss rapidly increases with decrease of loop antenna radius [27].

One challenge that arises in the design of magnetic antenna arrays is to achieve low intra-array coupling along with high gain. These two properties are essential for increasing the channel capacity in comparison to a single antenna communication system of comparable volume. In this light, this paper proposes a design based on circular loop antennas that avoids the gain reduction penalty associated with the multiple-pole loop designs. In addition, intra-array coupling cancellation is achieved by proper partial overlapping of the array elements, which stems from mutual magnetic flux cancellation. The mathematic approach employed in this paper considers each coil as a system of coupled inductors, where each inductor is a single turn loop. Both the self- and mutual-coil inductances are computed by summing the appropriate loop inductances. Then, a global optimization algorithm is employed to determine the coil locations and number of turns, to obtain the desired inductance and the minimal coupling between array elements. The proposed method allows to design a volume efficient, up to 3×3 array or a pyramidal shaped 4×4 array. It can be used in MIMO, or in multiple-frequency communication, and may be beneficial in applications where the channel capacity is low [28]. Results are validated experimentally, producing a volume efficient array with coupling coefficients between elements as low as 10^{-8} .

2. ANTENNA ARRAY COMMUNICATION METHODS

This section considers two communication methods that are used with antenna arrays, MIMO and multiple-frequency. The relative advantages and disadvantages of both are explained for the special case of the magnetic induction communication. It is shown that intra-array coupling cancellation is needed in both to increase the channel capacity, and that the multiple-frequency method becomes a viable candidate in high range applications. To demonstrate the attractiveness of the multiple-frequency method, we start by reviewing the basic relations of magnetic induction communication in order to illustrate why the operational bandwidth reduces when range increases, and to explain the opposing requirements of range and channel capacity. We then show the importance of minimal intra-array coupling in the multiple frequency communication method. This result is illustrated based on a 3×3 array.

With the MIMO method the data stream at each array element is different, but all elements operate at the same frequency band. This method works well in classic far electromagnetic field and in multiple-path rich environments. Under such conditions, the capacity of the array is linearly proportional to the number of array elements, provided the intra-array coupling is minimized [27, 29]. In magnetic induction communication, the field is a quasi-static and non-propagating, and hence no multiple path exists. This results in a rank deficient channel, similarly to conventional far field MIMO systems with

significant Line-of-Sight (LoS) components. In such situations the increase in capacity is not linearly proportional to number of array elements, and is significantly lower [29–32].

In contrast to MIMO, with the multiple-frequency method each antenna is fed with a different data stream, and operates at a different frequency band. Therefore, the channel capacity is linearly proportional to the number of the array elements, provided the required frequency band is available. Since increased range requires reduced bandwidth, the disadvantage of wider bandwidth in the multiple-frequency method diminishes at magnetic induction high range applications. Therefore, the multiple-frequency technique becomes more attractive in power limited, high range applications.

We now provide a brief review of magnetic induction communication equations that illustrate the basic relations between operational bandwidth and range. A typical SISO magnetic induction communication system includes the transmitting and receiving coils, series resonant capacitors, and load impedance, as illustrated in Fig. 1.

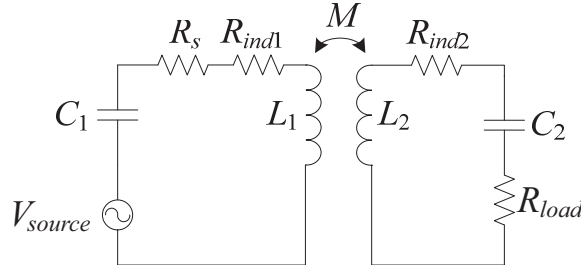


Figure 1. A typical magnetic induction communication circuit.

The efficiency of the transmitter and receiver is

$$\eta_T = \frac{R_s}{R_s + R_{ind1}} \tag{1}$$

$$\eta_R = \frac{R_{load}}{R_{load} + R_{ind2}}$$

where R_s and R_{load} are the source and load resistances, and $R_{ind1,2}$ are the transmitter and receiver coil resistances, respectively. The quality factor of the transmitter and receiver are

$$Q_T = \frac{\omega_0 L_1}{R_s + R_{ind1}} \tag{2}$$

$$Q_R = \frac{\omega_0 L_2}{R_{load} + R_{ind2}}$$

And power delivered to the load at resonance frequency is [33]

$$P_{L,res} = P_S \eta_T \eta_R Q_T Q_R k^2 \tag{3}$$

where P_s is the source power, and k is the coupling coefficient between the two coils. The communication range depends on the signal-to-noise ratio (SNR) at the receiver, which is proportional to received power and to quality factor of the transmitting and receiving circuits. Hence, at increased range, the operational bandwidth must be decreased.

The channel capacity is proportional to SNR and to bandwidth, which is inversely proportional to the quality factor. The channel capacity at the edge of communication bubble, where signal to noise ratio equals unity is

$$C = B_f f_0 \log_2 \left(1 + \frac{P_R}{N} \right) = B_f f_0 \log_2 2 = B_f f_0 \tag{4}$$

where the fractional bandwidth is defined by the higher quality factor of the transmitter and the receiver:

$$B_f = \frac{B}{f_0} = \min \left(\frac{1}{Q_T}, \frac{1}{Q_R} \right) \tag{5}$$

Hence the channel capacity is inversely proportional to the quality factor:

$$C = B_f f_0 = f_0 \cdot \min\left(\frac{1}{Q_T}, \frac{1}{Q_R}\right) \quad (6)$$

Observing Eqs. (3) and (6), it is clear that increased range and channel capacity are opposing requirements, so higher range requires higher quality factor, and the bandwidth is reduced.

To demonstrate the impact of the intra-array coupling on the multiple-frequency communication system, we consider a 3×3 array and examine the input impedance of the transmitters. It is shown that the input impedance of each transmitter is affected by the adjacent coils for high quality factors, when the intra-array coupling is not minimized. The coupling between the array elements is chosen to be 0.019. Such coupling coefficient is the average value of coupling between two coplanar coils with axes separated at $1.1D_{out}$, where D_{out} is the outer coil diameter, for wide range of number of layers and number of turns in each layer, as shown in Fig. 2.

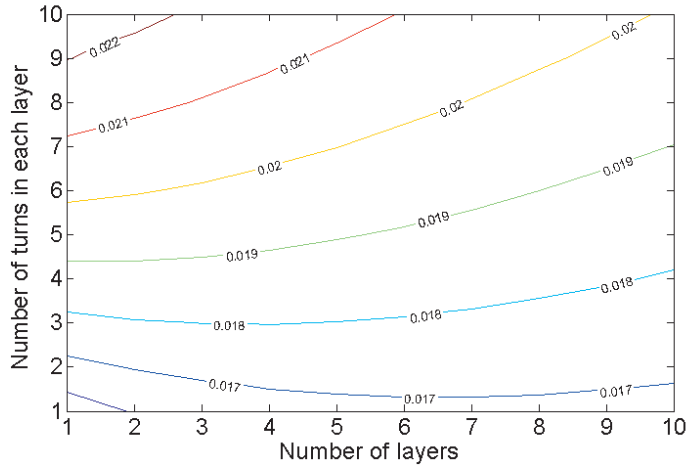


Figure 2. Coupling coefficient between two coils for varying number of layers and turns in each layer. The axes separation is $1.1D_{out}$.

The resonant frequencies of the three transmitters $f_{0,1}$, $f_{0,2}$, and $f_{0,3}$ are separated based on the 3 dB bandwidth:

$$f_{0,3} - f_{0,2} = f_{0,2} - f_{0,1} = BW = f_0/Q \quad (7)$$

where Q is the quality factor of the resonant circuit, and BW is the 3 dB bandwidth. Spice simulations reveal that such coupling coefficient between the adjacent coils is adequate when working with low quality factors, such as $Q = 10$. In such case the input impedances of the three transmitters are not affected by the mutual coupling due to large central frequency spacing, as shown in Fig. 3(a). However, for increased range operation, high quality factor is required, and in such case, the mutual coupling of the array elements limits the performance, as shown in Fig. 3(b) for $Q = 100$. Therefore, for both MIMO and multiple-frequency communication, the intra-array coupling must be diminished to achieve high capacities.

3. THE PROPOSED ARRAY TOPOLOGY

This section shows the proposed approach of reducing the intra-array coupling using flux cancellation. A number of coil topologies, such as thin and thick solenoids and flat coils are investigated, with an objective to identify volume efficient configurations. Finally, an optimization procedure is proposed to obtain the minimal intra array coupling for a required inductance of the array elements.

The proposed approach relies on flux cancellation in two partially overlapping loops. This principle is illustrated in Fig. 4(a). When the loops are located at a certain distance p , the upward directed flux

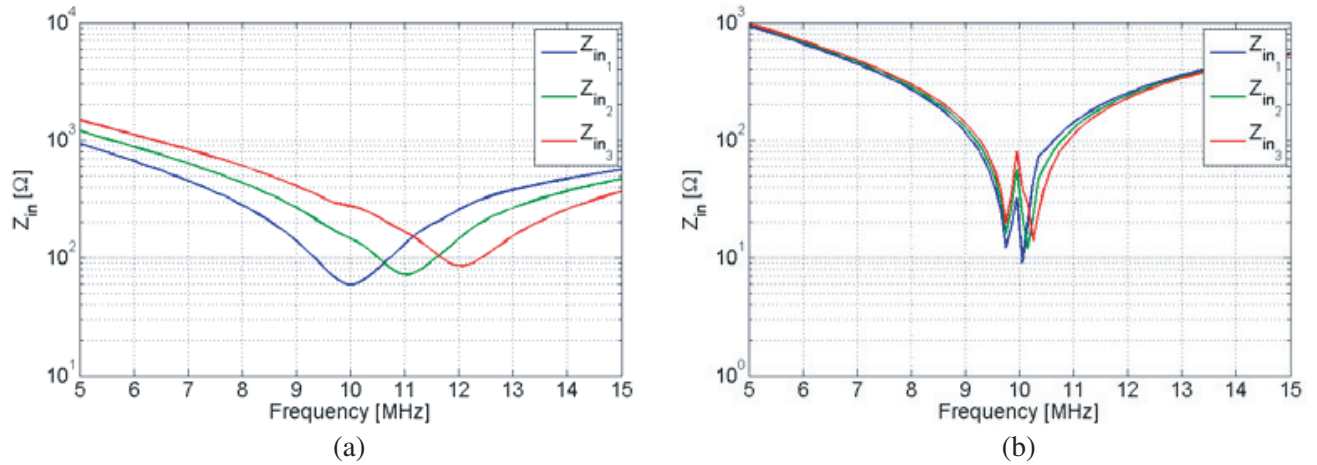


Figure 3. Input impedances of the three transmitters for (a) low quality factor: $Q = 10$, and (b) higher quality factor: $Q = 100$.

of coil 2 crossing coil 1 is cancelled by the downward directed flux of coil 2, resulting in zero net flux crossing coil 1. Such arrangement can be used for up to three coils in a nearly flat structure, as no more than three points can have identical distances between each one on a plane, as shown in Fig. 4(b). This principle can also be applied to four elements, resulting in a 4×4 array. This requires a three-dimensional structure forming a pyramid, with identical distances between each element, as shown in Fig. 4(c).

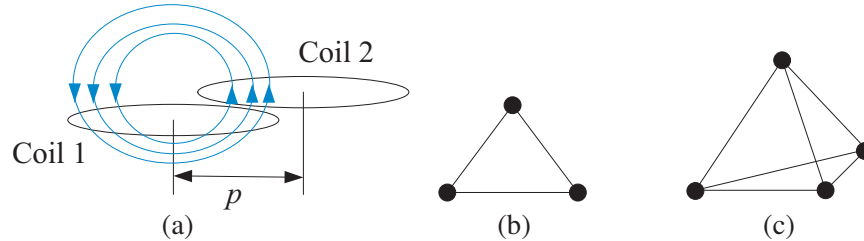


Figure 4. (a) Magnetic flux cancellation principle, (b) flat array arrangement with dots depicting loop centers, and (c) three-dimensional array arrangement with dots depicting loop centers.

When complete coils and no single turn loops are considered, the optimal distance between coils varies from the optimal one found for two loops. Therefore, an approach to compute the coupling coefficient between two complete coils is described next. The method is based on considering each coil as a system of coupled inductors, where each inductor is composed of a single turn loop. The self-inductance of each turn is computed according [34]:

$$L_{loop} = \mu R \left(\ln \left(\frac{8R}{r} \right) - 2 \right) \tag{8}$$

where R is the loop radius, and r is the wire radius. The self inductance of a complete coil requires computing mutual inductance of coaxial loops. The formula most frequently employed for this task is [35]:

$$M_{21} = \mu \frac{\sqrt{R_1 R_2}}{k} [(2 - k^2) K(k) - 2E(k)] \tag{9}$$

$$k = \sqrt{\frac{4R_1 R_2}{(R_1 + R_2)^2 + (z_2 - z_1)^2}}$$

where R_1 and R_2 are the loop radii; K and E are the complete elliptic integrals of the first and second kinds; z_1 and z_2 are the heights of the loops, respectively. This expression is limited to coaxial case, and hence for mutual inductance between coils, the general formula that employs Bessel functions is given [35]:

$$M_{21} = \mu\pi R_1 R_2 \int_0^\infty J_0(sp) J_1(sR_1) J_1(sR_2) e^{-s|z_2-z_1|} ds \quad (10)$$

where p is the axis pitch of the two loops, and $z_2 - z_1$ is the vertical distance between the loops, as illustrated in Fig. 5. The disadvantage of Equation (10) is that the integral is highly oscillatory, and even today its evaluation is much more time consuming than that of Eq. (9). The more numerically robust alternative to Eq. (10) is given in [36]:

$$\begin{aligned} M_{21} &= \frac{2\mu_0 R_1 R_2}{\pi} \int_0^\pi \frac{\cos\phi K(\widehat{k}(\phi)) d\phi}{\sqrt{(p + \chi(\phi))^2 + (z_2 - z_1)^2}} \\ \chi(\phi) &= \sqrt{R_1^2 + R_2^2 - 2R_1 R_2 \cos\phi} \\ \widehat{k}(\phi) &= \sqrt{\frac{4p\chi(\phi)}{(p + \chi(\phi))^2 + (z_2 - z_1)^2}} \end{aligned} \quad (11)$$

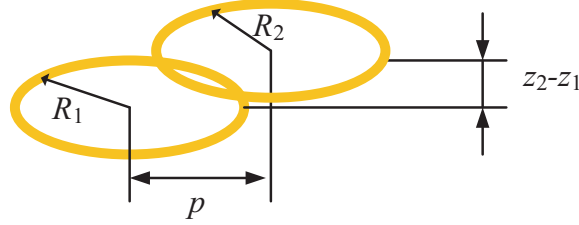


Figure 5. Geometry of two coupled loops with axis pitch p and vertical displacement $z_2 - z_1$.

To compute the self and mutual loop inductances of entire, multiple-turn coils, the self and mutual inductances of individual loops are represented in a matrix form, and the total coil self-inductance can be computed by summing all of the matrix entries related to this coil. The mutual inductance between two coils can be computed by summing all the mutual entries in the matrix. The self-inductance of a coil consisting of N_1 turns is computed by:

$$L_{self} = \sum_{i=1}^{N_1} \sum_{j=1}^{N_1} M_{ij}^{(self)} \quad (12)$$

where $M^{(self)}$ is a matrix consisting of self-inductances of the loops and loop-to-loop inductances of the coil. The mutual inductance between two coils consisting of N_1 and N_2 turns is:

$$M = \frac{1}{2} \sum_{i=1}^{N_1+N_2} \sum_{j=1}^{N_1+N_2} M_{ij}^{(mutual)} \quad (13)$$

where $M^{(mutual)}$ is a matrix consisting of loop-to-loop inductances of the two coils.

Next, we demonstrate the coupling coefficients of the three partially overlapping coils, composing an array, as a function of the axis pitch p and the vertical displacement between them. The considered configurations include thin and thick solenoids, and flat coils. The considered array is schematically illustrated in Fig. 6. As discussed previously, the coupling coefficient between each two coils has a deep notch at a certain distance. In this simulation, the coils parameters are as follows: the inner radius is 4 cm, wire diameter is 0.5 mm, and wire pitch factor is 1.1. Due to the fact that minimal coupling occurs at partially overlapping coils, the coils are vertically displaced. The displacement between the top turn of the lower coil to the bottom turn of the upper coil is schematically depicted in Fig. 6 as h_{12} and h_{23} . The coupling coefficients of the array composed of the thin, single layer solenoids with 100 turns are

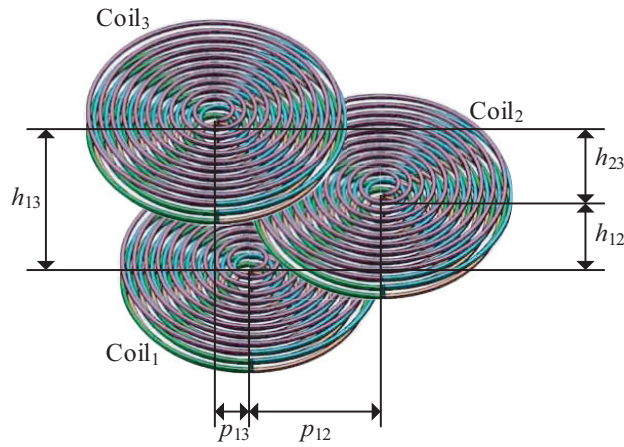


Figure 6. The considered communication arrays composed of the three coils.

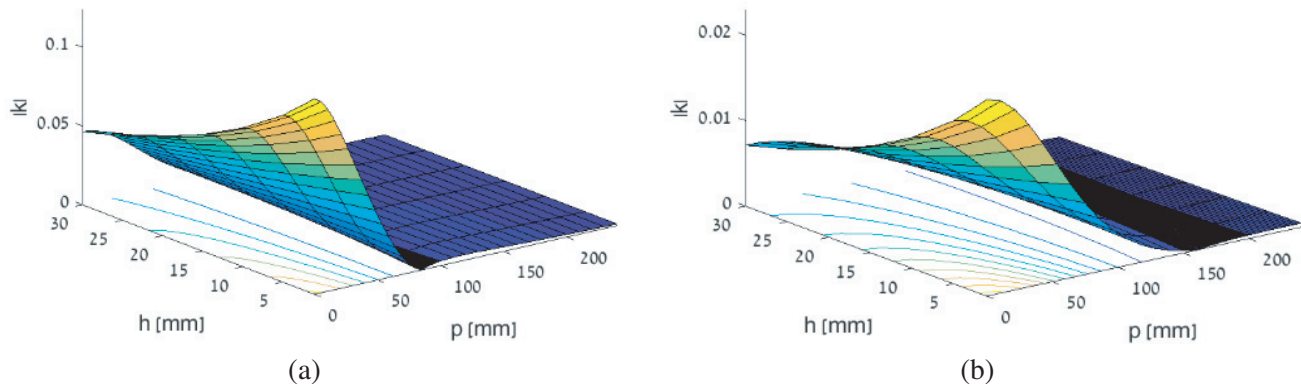


Figure 7. Coupling between two coils as function of axes pitch p and vertical spacing h . Each coil has 100 turns at a single layer. (a) Coupling between the bottom and the middle coils, and (b) coupling between the bottom and the top coils.

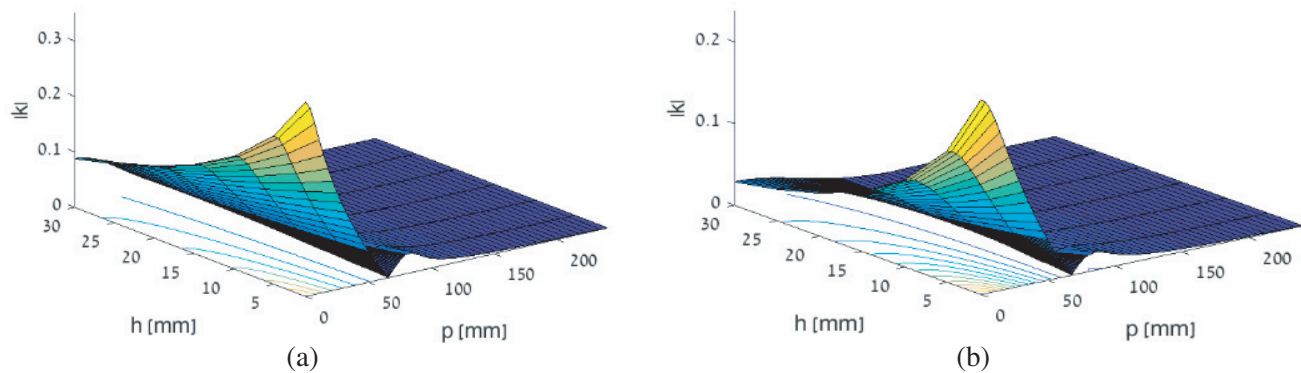


Figure 8. Coupling between two coils as function of axes pitch p and vertical spacing h . Each coil has 10 turns at 10 layers. (a) Coupling between the bottom and the middle coils, and (b) coupling between the bottom and the top coils.

shown in Fig. 7. The coupling coefficients of the thick solenoids with 10 layers and 10 turns per layer are shown in Fig. 8, and the coupling coefficients of the flat coils with 100 turns are shown in Fig. 9.

The results are validated by the CST Microwave Studio package for the case of a planar coil with 10 turns (Fig. 10). The results are in good matching with the analytic solution, and demonstrate a

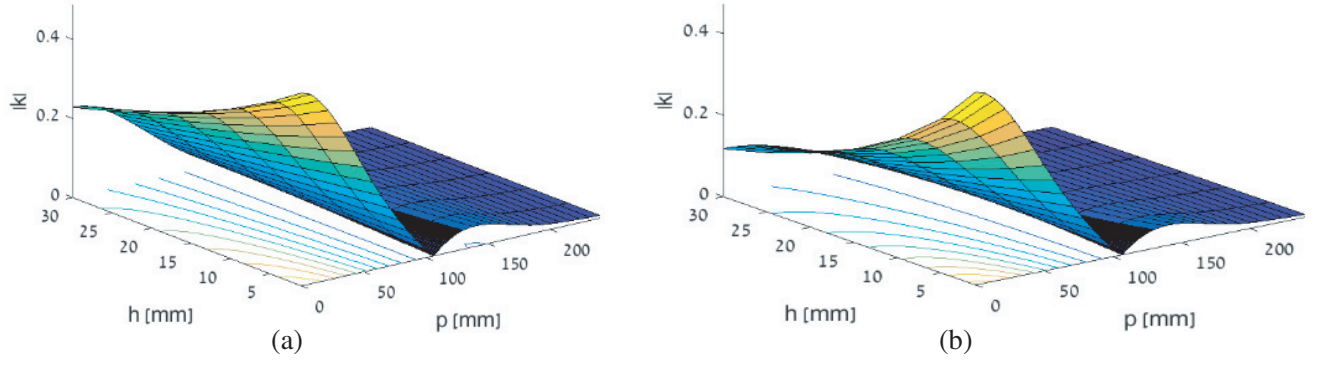


Figure 9. Coupling between two coils as function of axes pitch p and vertical spacing h . Each coil is a flat coil with 100 turns. (a) Coupling between the bottom and the middle coils, and (b) coupling between the bottom and the top coils.

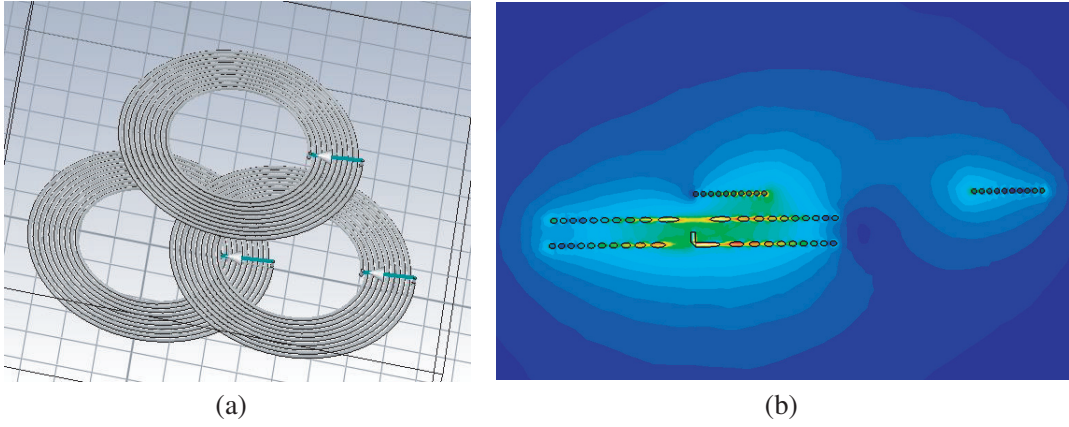


Figure 10. CST simulation of the flat coils with 10 turns. (a) The coils setup, (b) the cross sectional magnetic field.

coupling coefficient between the coils of 10^{-5} .

At all considered cases, the minimal coupling coefficient is below 10^{-4} for vertical spacing below 5 mm, which results in virtually orthogonal coils that are required for efficient MIMO or multiple-frequency array operation. It can be concluded by observing Fig. 7–Fig. 9 that the compactness of the array, and the minimal achievable coupling, depend on the coil geometries. It can be seen that the array constituted of thick, multiple layer solenoid coils, results in the most compact arrangement.

For high range applications, where a high quality factor is required, the minimal coupling may be obtained by solving an optimization problem, in which the coil inductance serves as a constraint:

$$\begin{aligned} \min : & |k_{12}| + |k_{13}| \\ \text{st. } & L_{\text{required}} - L(n_x, n_y) = 0 \end{aligned} \quad (14)$$

where n_x is the number of layers, and n_y is the number of turns in each layer. Explicitly, this optimization is defined as:

$$\min \frac{1}{2} \left| \sum_{l=1}^{2N} \sum_{m=1}^{2N} \frac{2\mu R_l R_m}{\pi} \int_0^\pi \frac{\cos \phi K \left(\sqrt{\frac{4p_{12} \sqrt{R_l^2 + R_m^2} - 2R_l R_m \cos \phi}{(p_{12} + \sqrt{R_l^2 + R_m^2} - 2R_l R_m \cos \phi)^2 + (z_l - z_m)^2}} \right)}{\sqrt{(p_{12} + \sqrt{R_l^2 + R_m^2} - 2R_l R_m \cos \phi)^2 + (z_l - z_m)^2}} d\phi \right| \quad (15)$$

$$\left. + \frac{1}{2} \sum_{l=1}^{2N} \sum_{n=1}^{2N} \frac{2\mu R_l R_m}{\pi} \int_0^\pi \frac{\cos \phi K \left(\frac{4p_{13} \sqrt{R_l^2 + R_n^2 - 2R_l R_n \cos \phi}}{\sqrt{(p_{13} + \sqrt{R_l^2 + R_n^2 - 2R_l R_n \cos \phi})^2 + (z_l - z_n)^2}} \right)}{\sqrt{(p_{12} + \sqrt{R_l^2 + R_m^2 - 2R_l R_m \cos \phi})^2 + (z_l - z_m)^2}} d\phi \right.$$

$$\text{st. } L_{required} = \sum_{i=1}^N \sum_{j=1}^N \mu \frac{\sqrt{(R_i + R_j)^2 + (z_i - z_j)^2}}{4\sqrt{R_i R_j}} \left[\left(2 - \frac{(4R_i R_j)^2}{(R_i + R_j)^2 + (z_i - z_j)^2} \right) \cdot K \left(\frac{4R_i R_j}{\sqrt{(R_i + R_j)^2 + (z_i - z_j)^2}} \right) - 2E \left(\frac{4R_i R_j}{\sqrt{(R_i + R_j)^2 + (z_i - z_j)^2}} \right) \right] \quad (16)$$

where three identical coils with $N = n_x n_y$ turns are assumed. The indices i and j belong to the same coil, while the indices l and m belong to the first and second coils, respectively, and indices l and n belong to the first and third coils. The optimization minimizes the coupling between the three coils, subject to a certain required self-inductance. The internal radius of the coil is chosen based on the

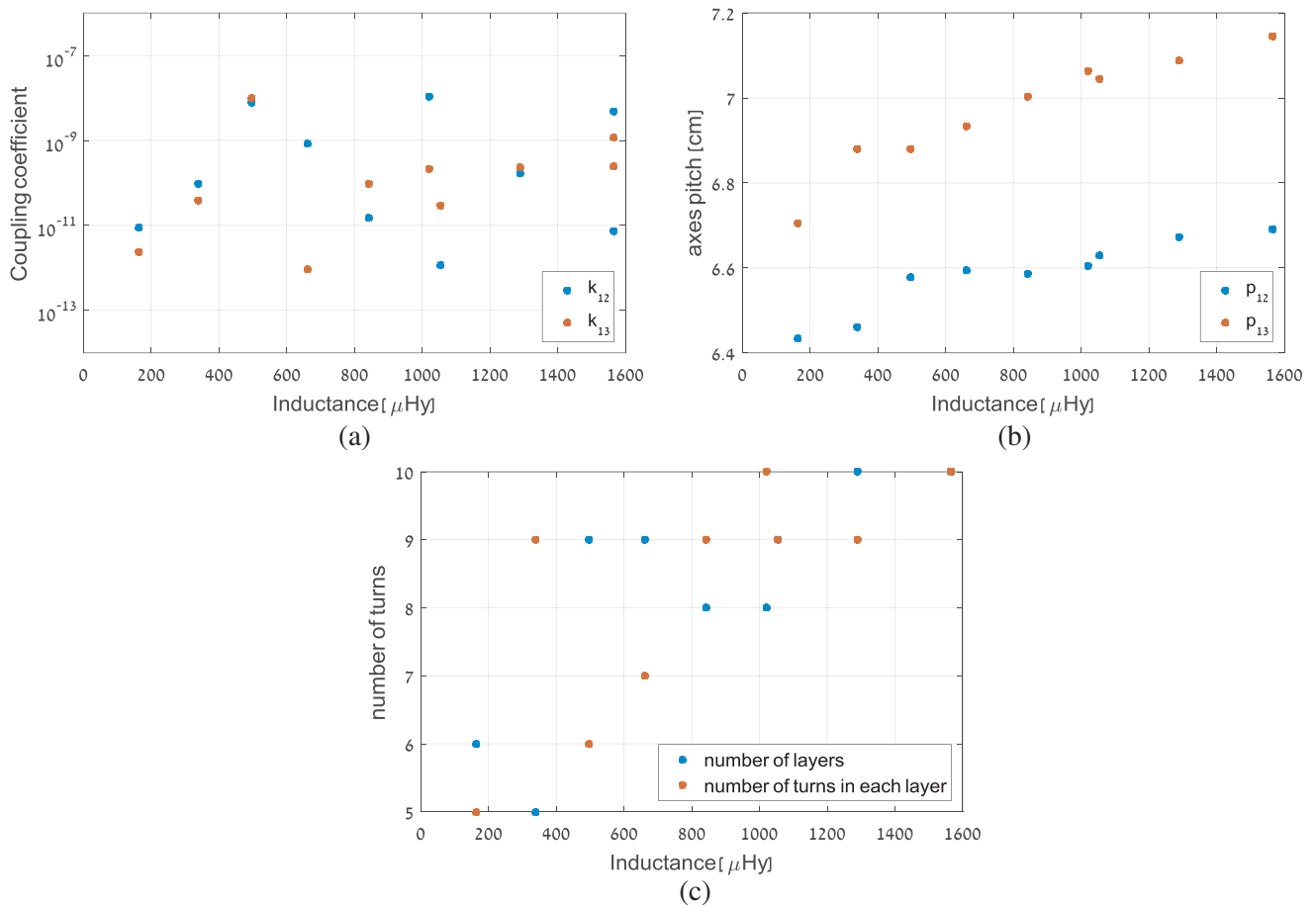


Figure 11. (a) Minimal coupling between two coils, (b) axis pitches at the minimally coupled array, and (c) number of turns of the optimal coils for the minimally coupled array.

application, and the radii of the loops constituting the coil are determined by the internal radius and the wire diameter. The optimization provides the optimal number of turns per layer n_y and number of layers n_x , and the optimal pitches between the coils axes p_{12} and p_{13} . This optimization problem is solved using a particle swarm Matlab solver.

The simulation results for ten coil values, spaced between $155 \mu\text{Hy}$ and $1550 \mu\text{Hy}$ are summarized at Fig. 11: the coupling coefficient is shown in Fig. 11(a), the axis pitches of the array elements are shown in Fig. 11(b), and the resulting number of turns as function of inductance is shown in Fig. 11(c).

4. EXPERIMENTAL RESULTS

The first experiment validates the minimal coupling between three array elements, and the second experiment illustrates the signals received in the minimally intra-array coupling system, and compares it to the signals received in a standard array. This is done with a multiple-frequency system, as it enables an easy visualisation of the benefit produced by the minimally coupled array.



Figure 12. A minimally coupled array of three coils.

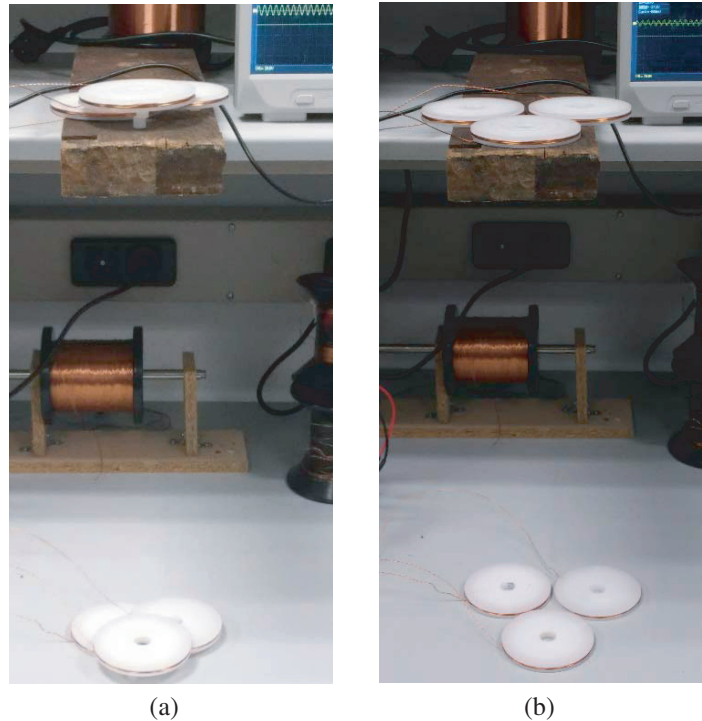


Figure 13. Communication setup utilizing (a) minimally coupled array and (b) a standard array.

Three identical coils are wound on a bobbin with inner radius of 4 cm. Each coil has 6 turns per layer, 9 layers, utilizing wire with diameter of 0.5 mm. The measured inductance is 502 μ Hy. The coils are resonated with series capacitors of 56 nF at 30 kHz, and arranged in a volume efficient array, as shown in Fig. 12. The low coupling between the coils in the array requires injection of high current into the transmitting coil. The frequency limitation of the employed AE Techron 2105 amplifier, leads to setting the injection frequency of 30 kHz. The coupled signal was measured by a spectrum analyzer. The coil locations are gradually varied to locate the minimum coupling point. The resultant axes pitch between the bottom/middle and middle/top coils is 6.6 cm, and the axes pitch between the bottom/top coils is 6.9 cm. The measured power is -92 dBm for adjacent coils, and -95 dBm for bottom to top coils. The excitation current was 5 A, supplied for short amount of time to prevent overheating of the coils. These measured power levels translate to coupling coefficients k_{12} and k_{13} of 1.2×10^{-8} , and 8.4×10^{-9} , respectively, which is worse than the simulation results. However, such low coupling coefficients, result in uncoupled coils in any practical communication system.

The second experiment emulates the multiple-frequency communication system. Towards this end, two identical arrays are placed at the distance of 50 cm. as shown in Fig. 13. The three transmitting coils are resonated by series capacitors of 56 nF, parallel combination of two 110 nF, and triple parallel combination of 160 nF, to resonate at 30 kHz, 30.3 kHz, and 30.6 kHz, respectively. The quality factors of the resonant circuits are approx. 100. The three coils are excited at appropriate resonance frequencies, and the received signals are measured by an oscilloscope. The waveforms are downloaded and FFT is performed at Matlab, due to scope FFT resolution limitation of 500 kHz/div. The results are illustrated at Fig. 14 for both the minimally coupled array and for the standard array. Observing Fig. 14, it can be easily concluded that the received signals with minimally coupled array enable distinguishing the different signals, while the signals received by a standard array strongly interfere each other.

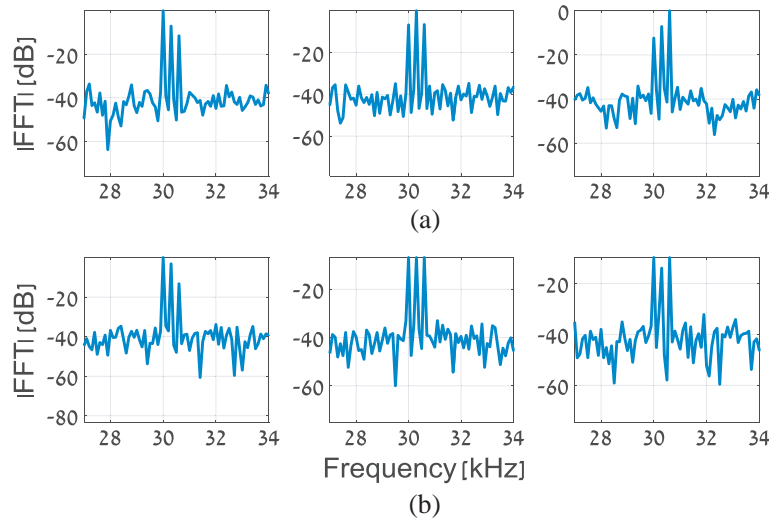


Figure 14. FFT of received signals at (a) minimally coupled array, and (b) a standard array.

5. CONCLUSIONS

Magnetic induction communication systems are a viable alternative to far field EM communication in challenging environments. However, due to the rapid decay of the near field with distance, these systems suffer from short range and low channel capacity. In this paper we propose a method to increase the channel capacity at a given range using an antenna array. The proposed method allows to reduce the coupling between the array elements, which is essential in both MIMO and multiple-frequency communication approaches. This is achieved by circular loop antennas, with proper partial overlapping that reduces the intra-array coupling due to magnetic flux cancellation. The mathematic approach employed to design this array considers each coil as a system of coupled inductors, where each

inductor is a single turn loop, and the total coil self and mutual inductances are computed by summing the appropriate single turn loop inductances. Volume efficient coil topologies are identified, and an optimization is proposed to minimize the intra-array coupling subject to a required inductance. The proposed method allows to design volume efficient, up to 3×3 , array, or pyramidal shaped 4×4 arrays. The designed array is verified experimentally, and intra-array coupling coefficients as low as 10^{-8} are measured. In addition, the designed array is tested with a high- Q multiple-frequency communication scheme to show the lack of intra-array interference. This result is compared to a standard array, which severely suffers from this interference. The proposed method can be applied in a variety of magnetic induction communication systems that require higher channel capacity or higher range, such as underground, underwater, and bio-medical applications.

REFERENCES

1. Sun, Z. and I. F. Akyildiz, "Magnetic induction communications for wireless underground sensor networks," *IEEE Transactions on Antennas and Propagation*, Vol. 58, No. 7, 2426–2435, 2010.
2. Sun, Z., P. Wang, M. C. Vuran, M. A. Al-Rodhaan, A. M. Al-Dhelaan, and I. F. Akyildiz, "Mise-pipe: Magnetic induction-based wireless sensor networks for underground pipeline monitoring," *Ad Hoc Networks Journal*, Vol. 9, No. 3, 218–227, Elsevier, 2011.
3. Tan, X. and Z. Sun, "An optimal leakage detection strategy for underground pipelines using magnetic induction-based sensor networks," *International Conference on Wireless Algorithms, Systems, and Applications*, 414–425, Springer, 2013.
4. Tariq, A. K., A. T. Ziyad, and A. O. Abdullah, "Wireless sensor networks for leakage detection in underground pipelines: A survey," *Procedia Computer Science*, Vol. 21, 491–498, 2013.
5. Sun, Z. and B. Zhu, "Channel and energy analysis on magnetic induction-based wireless sensor networks in oil reservoirs," *IEEE International Conference on Communications (ICC)*, 1748–1752, 2013.
6. Agbinya, J. I., *Principles of Inductive Near Field Communications for Internet of Things*, River Publishers, Denmark, 2011, ISBN: 978-87-92329-52-3.
7. Sun, Z. and I. F. Akyildiz, "Underground wireless communications using magnetic induction," *Proc. IEEE International Conference on Communications (ICC)*, 1–5, 2009.
8. Akyildiz, I. F. and E. P. Stuntebeck, "Wireless underground sensor networks: Research challenges," *Ad Hoc Networks Journal*, Vol. 4, 669–686, Elsevier, 2006.
9. Li, L., M. C. Vuran, and I. F. Akyildiz, "Characteristics of underground channel for wireless underground sensor network," *Proc. Med-Hoc Net*, Corfu, Greece, Jun. 2007.
10. Agbinya, J. I., "Investigation of near field inductive communication system models, channels and experiments," *Progress In Electromagnetics Research B*, Vol. 49, 129–153, 2013.
11. Agbinya, J. I., N. Selvaraj, A. Ollett, S. Ibos, Y. Ooi-Sanchez, M. Brennan, and Z. Chaczko, "Characteristics of the magnetic bubble 'Cone of Silence' in near-field magnetic induction communications terminals," *Journal of Battlefield Technology*, Vol. 13, No. 1, 21–25, Mar. 2010.
12. Sun, Z. and I. F. Akyildiz, "Deployment algorithms for wireless underground sensor networks using magnetic induction," *Global Telecommunications Conference (GLOBECOM)*, 1–5, IEEE, 2010.
13. Domingo, M., "Magnetic induction for underwater wireless communication networks," *IEEE Transactions on Antennas and Propagation*, Vol. 60, No. 6, 2929–2939, 2012.
14. Masihpour, M., D. Franklin, and M. Abolhasan, "Multipleshop relay techniques for communication range extension in near-field magnetic induction communication systems," *Journal of Networks*, Vol. 8, No. 5, 2013.
15. Akyildiz, I., Z. Sun, and M. Vuran, "Signal propagation techniques for wireless underground communication networks," *Physical Communication*, Vol. 2, No. 3, 167–183, 2009.
16. Sun, Z. and I. Akyildiz, "Optimal deployment for magnetic induction-based wireless networks in challenged environments," *IEEE Transactions on Wireless Communications*, Vol. 12, No. 3, 996–1005, 2013.

17. Kisseleff, S., I. Akyildiz, and W. Gerstacker, "Throughput of the magnetic induction based wireless underground sensor networks: Key optimization techniques," *IEEE Transactions on Communications*, Vol. 62, No. 12, 4426–4439, 2014.
18. Akyildiz, I. F., P. Wang, and Z. Sun, "Realizing underwater communication through magnetic induction," *IEEE Communications Magazine*, Vol. 53, No. 11, 42–48, 2015.
19. Coillot, C., J. Moutoussamy, R. Lebourgeois, S. Ruocco, and G. Chanteur, "Principle and performance of a dual-band search coil magnetometer: A new instrument to investigate fluctuating magnetic fields in space," *IEEE Sensors J.*, Vol. 10, No. 2, 255–260, 2010.
20. Grosz, A., E. Paperno, S. Amrusi, and B. Zadov, "A three-axial search coil magnetometer optimized for small size, low power, and low frequencies," *IEEE Sensors J.*, Vol. 11, No. 4, 1088–1094, 2011.
21. Lukoschus, D., "Optimization theory for induction-coil magnetometers at higher frequencies," *IEEE Transactions on Geoscience Electronics*, Vol. 17, No. 3, 56–63, 1979.
22. Grosz, A. and E. Paperno, "Analytical optimization of low-frequency search coil magnetometers," *IEEE Sensors J.*, Vol. 12, No. 8, 2719–2723, 2012.
23. Cavoit, C., "Closed loop applied to magnetic measurements in the range 1 of 0.1–50 MHz," *Rev. Sci. Instrum.*, Vol. 77, No. 6, 2006, <http://dx.doi.org/10.1063/1.2214693>.
24. Tal, N., Y. Morag, and Y. Levron, "Increasing the sensitivity of search coil magnetometer by capacitive compensation," *IEEE Sensors J.*, Vol. 16, No. 12, 4671–4672, 2016.
25. Nguyen, H., J. I. Agbinya, and J. Devlin, "Channel characterisation and link budget of MIMO configuration in near field magnetic communication," *Int. J. Electron. Telecommun.*, Vol. 59, No. 3, 255–262, Aug. 2013.
26. Gottula, R. B., "Discrete-time implementation antenna design and MIMO for near-field magnetic induction communications," 2012, <http://hdl.lib.byu.edu/1877/etd5440>.
27. Kim, H. J., J. Park, K. S. Oh, J. P. Choi, J. E. Jang, and J. W. Choi, "Near-field magnetic induction MIMO communication using heterogeneous multipole loop antenna array for higher data rate transmission," *IEEE Transactions on Antennas and Propagation*, Vol. 64, No. 5, 1952–1962, 2016.
28. Yenchek, M. R., G. T. Homce, N. W. Damiano, and J. R. Srednicki, "NIOSH-sponsored research in through-the-Earth communications for mines: A status report," *IEEE Transactions on Industry Applications*, Vol. 48, No. 5, 1700–1707, 2012.
29. Sarris, I. and A. R. Nix, "Design and performance assessment of high-capacity MIMO architectures in the presence of a line-of-sight component," *IEEE Transactions on Vehicular Technology*, Vol. 56, No. 4, 2194–2202, 2007.
30. Yu, K., M. Bengtsson, B. Ottersten, and M. Beach, "Narrowband MIMO channel modeling for LOS indoor scenarios," *Proc. XXVIIIth Trienn. Gen. Assem. Int. URSI*, Aug. 2002.
31. Cottatellucci, L. and M. Debbah, "On the capacity of MIMO rice channels," *Proc. 42nd Allerton Conf.*, 1506–1516, 2004.
32. Sakaguchi, K., H. Y. E. Chua, and K. Araki, "MIMO channel capacity in an indoor line-of-sight (LOS) environment," *IEEE Transactions on Communications*, Vol. E88-B, No. 7, 3010–3019, Jul. 2005.
33. Agbinya, J. I. and M. Masilpour, "Power equations and capacity performance of magnetic induction communication systems," *Wireless Pers. Commun.*, Vol. 64, 831–845, 2012.
34. Elliot, R. S., "Electromagnetics in free space," *Electromagnetics*, Ch. 5, 314, McGraw-Hill, 1966.
35. Conway, J. T., "Inductance calculations for noncoaxial coils using Bessel functions," *IEEE Trans. Mag.*, Vol. 43, No. 3, 1023–1034, 2007.
36. Conway, J. T., "Mutual inductance for an explicitly finite number of turns," *Progress In Electromagnetics Research B*, Vol. 28, 273–287, 2011.